

## Folded-optics-based quartz-enhanced photoacoustic and photothermal hybrid spectroscopy

### ARTICLE INFO

#### Keywords

Photoacoustic spectroscopy  
Photothermal spectroscopy  
Multi-pass cell  
Quartz tuning fork

### ABSTRACT

Folded-optics-based quartz-enhanced photoacoustic and photothermal hybrid spectroscopy (FO-QEPA-PTS) is reported for the first time. In FO-QEPA-PTS, the detection of the photoacoustic and photothermal hybrid signal is achieved through the use of a custom quartz tuning fork (QTF), thereby mitigating the issue of resonant frequency mismatch typically encountered in quartz-enhanced photoacoustic-photothermal spectroscopy employing multiple QTFs. A multi-laser beam, created by a multi-pass cell (MPC) with a designed single-line spot pattern, partially strikes the inner edge of the QTF and partially passes through the prong of the QTF, thereby generating photoacoustic and photothermal hybrid signals. To assess the performance of FO-QEPA-PTS, 1 % acetylene is selected as the analyte gas and the  $2f$  signals produced by the photoacoustic, the photothermal, and their hybrid effects are measured. Comparative analysis against QEPAS and QEPTS reveals signal gain factors of  $\sim 79$  and  $\sim 14$ , respectively, when these laser beams created by MPC excite the QTF operating at fundamental resonance mode in phase. In the FO-QEPA-PTS signal, the proportions of the photoacoustic and the photothermal effects induced by the multiple beams are  $\sim 7\%$  and  $93\%$ , respectively.

### 1. Introduction

Cost-effective gas sensing systems play critical roles in numerous field applications, such as environmental monitoring, medical diagnostic, and homeland security, due to their ability to identify target trace gases with high sensitivities [1–4]. Quartz tuning fork (QTF)-based sensors offer great promise for such gas sensing systems, thanks to their small size, simple design, and potentially low cost [5–7]. In particular, quartz-enhanced photoacoustic spectroscopy (QEPAS) has gained significant popularity as a well-established technique that utilizes a QTF. In QEPAS, a modulated laser beam is directed through the QTF prongs where it interacts with the target analyte surrounding the QTF. This interaction leads to cyclic heating and cooling of the analyte. Subsequently, thermal disturbances induce the generation of an acoustic pressure wave through vibration-to-translational (V-T) relaxation processes, thereby causing the QTF tines to oscillate reciprocally [8,9]. Notably, this excitation induces an in-lane anti-symmetrical vibration mode in the QTF [10]. As a result, the QTF can be characterized as an acoustic quadrupole exhibiting robust immunity to external environmental sounds [11–13]. The other QTF-based sensing technique is called by quartz-enhanced photothermal spectroscopy (QEPTS) [14–16]. In QEPTS, the QTF serves as a photothermal detector, which is distinct from QEPAS [17–19]. The absorption of laser energy by the QTF leads to a conversion of light energy to photothermal energy, causing thermoelastic expansion and deformation of the QTF. When the laser is modulated, the thermoelastic expansion induces mechanical vibration in the QTF. Furthermore, the resonant characteristic of the QTF causes the mechanical vibration to be resonant-enhanced when the modulation frequency matches the intrinsic frequency of the QTF. As a result of the piezoelectric effect, the light-induced mechanical vibration generates piezoelectric charges on the surface of the QTF, which are then converted to a piezoelectric signal [20].

To enhance the signal intensity of QEPTS, Ma et al. introduced multi-quartz-enhanced photothermal spectroscopy (M-QEPTS) in 2020 [21]. This technique utilizes two QTFs as photothermal detectors to amplify the photothermal signal generated within a 20-cm optical gas cell. To maximize the photothermal effects, two lenses are employed to focus the transmitted energy of the laser beam on the surface of the QTFs. The application of this high-energy-density irradiation effectively catalyzes the production of more robust photothermal effects. Nonetheless, challenges arise from the potential frequency deviations between the two QTFs and the intricacies inherent in the focusing system. These factors collectively impose limitations on the progression of this gas-sensing technique. In 2019, Zheng et al. proposed quartz-enhanced photothermal-acoustic spectroscopy, which attempted to combine QEPAS and QEPTS to make them work simultaneously and enhance signal intensity [14]. A QTF simultaneously measured the sound signals generated nearby through the photoacoustic effect and the photothermal signals excited by the light beam, which interacts with the analyte at an open-path length of 2-m from the laser source to the QTF. The application of this technique is greatly restricted due to the requirement of immersing the setup with a 2-m open length in the measurement environment.

In this paper, we present, for the first time, a spectroscopic technique called folded optics-based quartz-enhanced photoacoustic and photothermal hybrid spectroscopy (FO-QEPA-PTS). The concept behind FO-QEPA-PTS is to introduce folding in the optical path, allowing the laser beam to traverse the prongs of the QTF multiple times. This arrangement facilitates the creation of multiple detection points on the QTF for both photoacoustic and photothermal effects. The incorporation of a folded path allows for enhanced generation of photoacoustic and photothermal signals within a compact volume. To implement this idea, we require an optical cell that allows all light rays to remain within a single plane while maximizing the number of optical reflections. A large-

<https://doi.org/10.1016/j.pacs.2023.100580>

Received 18 October 2023; Received in revised form 21 November 2023; Accepted 2 December 2023

Available online 7 December 2023

2213-5979/© 2023 The Author(s). Published by Elsevier GmbH. This is an open access article under the CC BY-NC-ND license (<http://creativecommons.org/licenses/by-nc-nd/4.0/>).

prong-spacing QTF is inserted into the optical cell with the response positions of the QTF for FO-QEPA-PTS.

## 2. Experimental setup

The schematic diagram of the FO-QEPA-PTS gas sensing system is illustrated in Fig. 1. A MPC featuring a single-line spot pattern was designed, utilizing two spherical mirrors to refocus the beam shape within this cavity. To achieve an optimal MPC featuring a single-line spot pattern, the diameter and focal length of the spherical mirror of MPC were consistently set at 10 mm and 50 mm, respectively. The laser beam was incident on the input mirror at coordinates (0, 6.25 mm). Maintaining a mirror spacing of 36.6 mm and an incident angle of 5 degrees for the initial beam, we captured a photograph illustrating the designed single-line spot pattern, as shown in Fig. 1. The MPC facilitates the presence of 60 laser beams within its cavity, thereby increasing the absorbed energy of the analyte following Lambert-Beer Law. To reduce the response time [7,22], the MPC was designed with a volume of  $\sim 3$  mL and a mirror spacing of 36.6 mm. A custom quartz tuning fork (QTF) with a resonance frequency of 7.2 kHz was inserted into the MPC to serve as a detector. The Q factor of the QTF was measured to be 6020. The custom QTF utilized in this study had a prong length of 10 mm and a spacing of 800  $\mu\text{m}$ . These dimensions were chosen to ensure that all ray trajectories within the MPC remained partially within the gap of the QTF and illuminated partially its inner edge. A continuous wave (CW) fiber-coupled distributed feedback (DFB) diode laser was employed as a probe light source. A  $\text{C}_2\text{H}_2$  absorption line located at  $6529.17\text{ cm}^{-1}$  was selected when the operating current and temperature of this laser were controlled at 189 mA and  $35.5\text{ }^\circ\text{C}$  by a custom laser control circuit board (CCB) controller, respectively. The output power of the probe light source is 24 mW. To enhance the performance of the FO-QEPA-PTS sensing system, wavelength modulation spectroscopy with 2nd harmonic detection was implemented. A ramp signal, generated from the laptop, was used to scan the laser wavelength across the absorption line, while a sine wave signal dithers the laser wavelength at a frequency of 7.2 kHz. The output laser beam from the DFB laser was coupled into the designed MPC through a fiber collimator, which had a beam waist of  $\sim 500\text{ }\mu\text{m}$  at a working distance of 40 mm. The collimated laser beam was directed into the MPC and the output electric signal, generated by the piezoelectric effect in the QTF, was amplified using a low-noise transimpedance amplifier. Subsequently, the signal was transferred to a commercial lock-in amplifier (Stanford Research Systems, Model SR830) for further processing. The lock-in amplifier demodulated the signal in the  $2f$  mode relative to the sync signal, which was configured with a 12 dB/oct filter slope and a time constant ( $\tau$ ) of 1 s corresponding

to a detection bandwidth of 0.25 Hz. A Labview™ program was employed to control the experiment system, and the demodulated  $2f$  spectra was analyzed and displayed on the laptop.

## 3. Experimental results and discussions

Performances of the FO-QEPA-PTS sensor system were optimized by detecting a fixed concentration of 1 %  $\text{C}_2\text{H}_2$  in nitrogen ( $\text{N}_2$ ) gas mixture under atmospheric pressure and room temperature conditions. To avoid an additional noise, the gas flow rate in this system was set to 50 SCCM. Using  $2f$ -WMS-based FO-QEPA-PTS gas sensing, the signal amplitude was initially characterized by its dependence on the modulation depth of the laser since the maximum peak of the  $2f$  signal occurs at the optimal modulation depth [23]. In this sensor system, the spherical mirrors of the MPC were replaced with two high-transmission windows, forming a gas chamber and allowing the laser beam to pass through the QTF only once. The responses of the QEPAS and QEPA-PTS signals to different positions of the QTF were investigated, respectively. The cartesian coordinate system was established in Fig. 2, with the y-axis positioned at the center of the QTF prong spacing and the x-axis at the top edge of the QTF. A collimated laser beam was focused on point A, situated at the center of the QTF prong spacing and positioned  $\sim 1.2$  mm from the top of the QTF. This specific point exhibited a peak QEPAS response

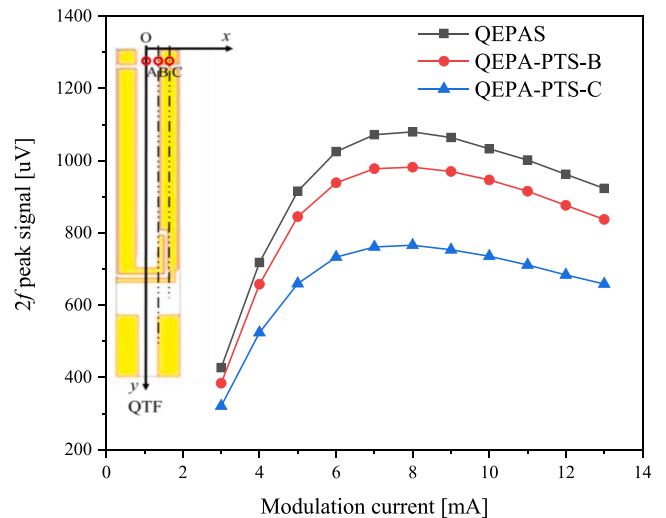


Fig. 2. Wavelength modulation depth dependence.

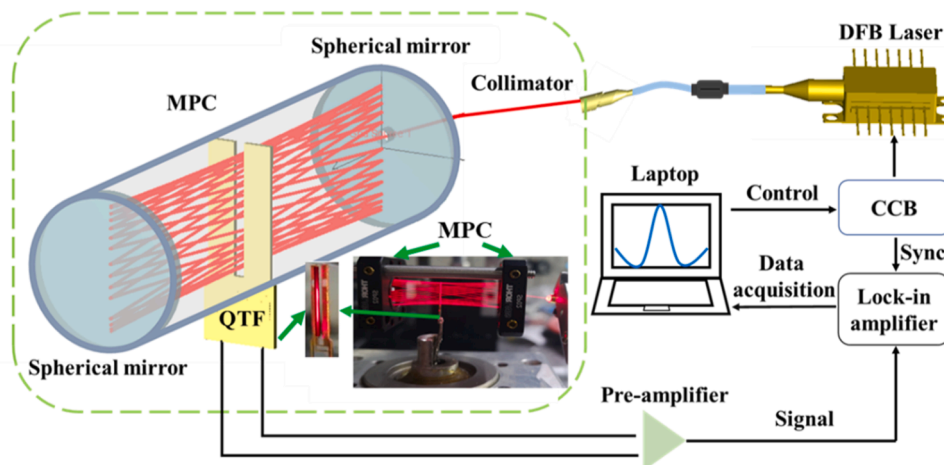


Fig. 1. FO-QEPA-PTS system configuration. Red lines: transmission of the laser beams between two identical spherical mirrors; QTF: quartz tuning fork; CCB: control circuit board. Insert photograph: beam trajectories generated by MPC touching QTF and passing through it.

attributed to the distinctive structure of the customized QTF [24]. Upon translating the laser beam along the x-axis to point B, positioned at the inner edge of the QTF prong and passing through it, the system exhibited the generation of the QEPA-PTS signal. Consequently, a  $2f$  peak signal was observed, registering a 10 % reduction compared to the corresponding QEPAS signal. When the laser beam along the x-axis to the point C, positioned at the center of the QTF prong, a minimum signal amplitude from QEPA-PTS was obtained, which aligns with the findings of previous studies [14]. The variation in signal amplitude is attributed to the electrode layer pattern on the surface of the QTF. A silver layer, characterized by high reflectivity for the laser beam, coats most of the area of the QTF prong [25]. However, there is no coating in the vicinity of the QTF edge, causing more photons to be absorbed by the QTF and resulting in a higher signal amplitude. These  $2f$  peak signals as a function of the modulation depth are presented in Fig. 2. The strongest  $2f$  signals for QEPAS and QEPA-PTS were observed when the modulation current was set to 8 mA under normal temperature and pressure conditions. This observation indicated the optimal optical modulation depth for the measurement of  $C_2H_2$ .

Given that the FO-QEPA-PTS signal is derived from the photoacoustic and photothermal hybrid effect in the system, and that the signals of QEPAS and QEPTS are dependent on the positioning of the laser focal point along both the symmetry axis (y-axis) and the inner edge of the QTF, respectively [26], it's crucial to optimize the positioning based on the output signals of QEPAS, QEPTS, and FO-QEPA-PTS. To achieve this, a three-dimensional linear stage with a typical step size of  $100\ \mu\text{m}$  was employed to precisely move the excited laser beam along the symmetry axis (y-axis) or the inner edge of the QTF in Fig. 2, spanning from the top (point a) to the bottom (point b), as depicted in Fig. 3. The signal amplitudes of both QEPAS and QEPA-PTS were plotted in Fig. 3 as a function of the vertical displacement of the excited laser beam. The highest signal amplitude for QEPAS (1.06 mV) and QEPA-PTS (6.10 mV) were obtained when the vertical displacement was  $\sim 1.2$  and 10 mm, respectively. The highest signal amplitude of QEPA-PTS was  $\sim 6$  times higher than that of QEPAS signal, as illustrated in Fig. 3.

To analyze the photothermal signal of the system, a reference cell filled with a 1 %  $C_2H_2/N_2$  mixture was placed in front of the gas chamber. The absorption path-length of the reference cell was half of the mirror spacing of the MPC  $\sim 18$  mm. The signal amplitudes of QEPTS were also plotted in Fig. 3 as a function of the vertical displacement of the excited laser beam when the gas chamber was filled with ambient nitrogen gas. The highest signal amplitude of QEPTS ( $\sim 6.10$  mV) was achieved at a vertical displacement of 10 mm. It is noteworthy that the highest signal amplitude of QEPTS and the corresponding position of the QTF were the same as those of QEPA-PTS. These findings confirm that the QEPA-PTS signal is generated through a combination of the photoacoustic and photothermal hybrid effects. The signal amplitude of QEPA-PTS is influenced by the photoacoustic effect at the top of the QTF and the photothermal effect near the base of the QTF. Furthermore, the signal amplitude of QEPA-PTS is equivalent to the addition of QEPTS and half of the QEPAS signal, as demonstrated in Fig. 3.

To enhance the hybrid photoacoustic and photothermal signal, the QTF was coupled into the MPC. The insertion depth of the QTF into the MPC was optimized by evaluating the output signal of FO-QEPA-PTS. The normalized signal amplitudes of FO-QEPA-PTS were plotted in Fig. 4 as a function of the vertical displacement of the MPC along the inner edge of the QTF (Line A), ranging from the top (point a) to the bottom (point b). The highest signal amplitude was achieved at a displacement of  $\sim 11$  mm. The corresponding  $2f$  signal peak measured at this position with a 1 %  $C_2H_2/N_2$  mixture is presented in Fig. 5, showing a value of 83.23 mV. Therefore, the signal gain factors of FO-QEPA-PTS compared to traditional QEPAS and QEPTS methods are  $\sim 79$  and  $\sim 14$ , respectively, as demonstrated in Fig. 3. Due to the fact there were no beams from 0 to 1 mm on the symmetry axis of the MPC, as illustrated in Fig. 4, the FO-QEPA-PTS peak signal was  $\sim 0$  in the moving distance of

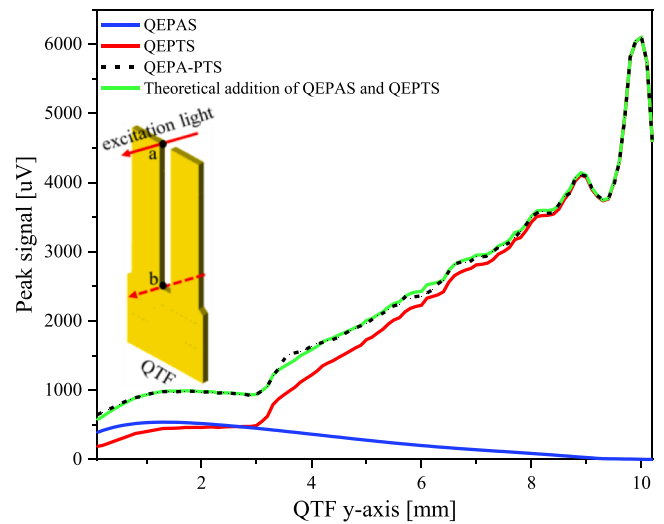


Fig. 3. Signal amplitudes from QEPA-PTS (black line segment), QEPAS (blue line), and QEPTS (red line) as functions of the laser focusing point from point a to point b along the QTF, respectively. A theoretical addition (green line) of QEPAS and QEPTS signal amplitudes.

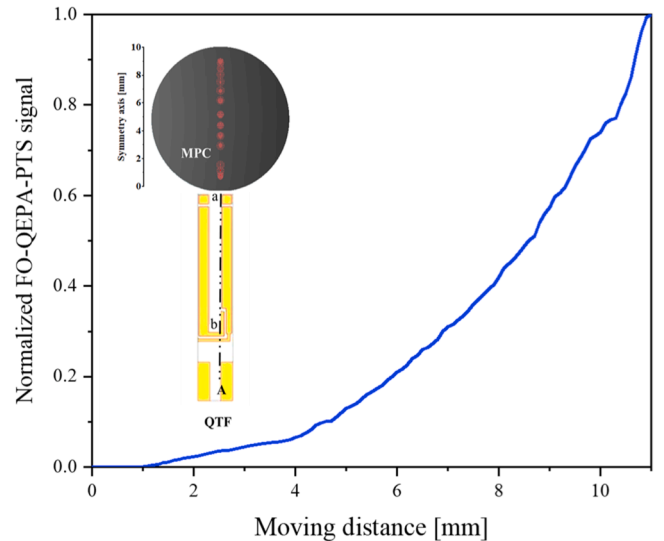


Fig. 4. Normalized FO-QEPA-PTS signal amplitudes as a function of the vertical moving distance of the single-line spot pattern-MPC.

0–1 mm.

It's crucial to investigate the contribution of the photoacoustic effect and the photothermal effect in this FO-QEPA-PTS system, as the FO-QEPA-PTS signal represents a hybrid of these two effects. In the FO-QEPA-PTS system, all 60 beams generated by this MPC are translated along the y-axis without intersecting the surface of the QTF. Consequently, the photoacoustic effect is selectively captured by the QTF, and the corresponding  $2f$  spectrum is displayed in Fig. 5. The FO-QEPA-PTS signal demonstrates a higher amplitude compared to FO-QEPAS, with a gain factor of  $\sim 7$ . Due to an approximate 50 % power loss of the laser beam when passing through the QTF for the first time, the actual gain factor of the FO-QEPA-PTS signal compared to FO-QEPAS is  $\sim 14$ . Therefore, in our proposed FO-QEPA-PTS system, the proportions of the photoacoustic effect and the photothermal effect are estimated to be  $\sim 7$  % and  $\sim 93$  %, respectively.

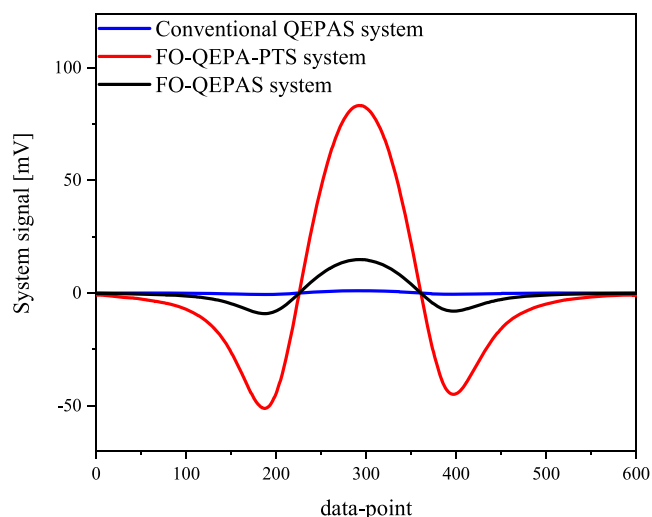


Fig. 5.  $2f$  signals of conventional QEPAS (blue line), FO-QEPA-PTS (red line), and FO-QEPAS (black line).

#### 4. Conclusions

In conclusion, we have successfully developed a FO-QEPA-PTS sensor utilizing a single-line pattern MPC and a custom QTF operating at its fundamental resonance mode. Unlike previously reported dual-tuning fork-based techniques such as QEPAS and QEPTS [26], our system allows for simultaneous detection of photoacoustic and photothermal signals generated by 60 sources. This eliminates the signal loss associated with frequency deviation in dual-QTF configurations. Consequently, we achieved remarkable signal gain factors of  $\sim 79$  and  $\sim 14$  compared to traditional QEPAS and QEPTS, respectively. Our proposed FO-QEPA-PTS system exhibits a distribution of  $\sim 7\%$  and  $\sim 93\%$  for the contributions of the photoacoustic and photothermal effect induced by the MPC, respectively. This signal amplitude of FO-QEPA-PTS can be further improved through an increase in the optical absorption length, as the photothermal signal is directly proportional to the absorption length. Moreover, FO-QEPA-PTS is better suited for operation at low pressure because the Q-factor of the QTF is higher at low pressure [26], resulting in a stronger photothermal signal.

#### CRediT authorship contribution statement

**Wu Hongpeng:** Funding acquisition, Supervision, Writing – review & editing. **Cui Ruyue:** Data curation, Formal analysis, Investigation, Methodology, Software, Supervision, Validation, Writing – original draft, Writing – review & editing. **Spagnolo Vincenzo:** Methodology, Supervision. **Tittel Frank K.:** Methodology, Supervision. **Dong Lei:** Funding acquisition, Investigation, Methodology, Supervision, Validation, Writing – review & editing. **Chen Weidong:** Investigation, Methodology, Supervision.

#### Declaration of Competing Interest

The authors declare that they have no known competing financial interests or personal relationships that could have appeared to influence the work reported in this paper.

#### Acknowledgements

The project is sponsored by National Key R&D Program of China (No. 2019YFE0118200); National Natural Science Foundation of China (NSFC) (Nos. 62235010, 62175137, 62122045, 62075119); The Shanxi Science Fund for Distinguished Young Scholars (20210302121003); The

High-end Foreign Expert Program (Nos. G2023004005L).

#### References

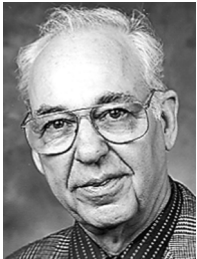
- [1] R. Cui, L. Dong, H. Wu, W. Ma, L. Xiao, S. Jia, W. Chen, F.K. Tittel, Three-dimensional printed miniature fiber-coupled multipass cells with dense spot patterns for ppb-level methane detection using a near-IR diode laser, *Anal. Chem.* 92 (19) (2020) 13034–13041.
- [2] R. Cui, L. Dong, H. Wu, S. Li, L. Zhang, W. Ma, W. Yin, L. Xiao, S. Jia, F.K. Tittel, Highly sensitive and selective CO sensor using a 2.33  $\mu\text{m}$  diode laser and wavelength modulation spectroscopy, *Opt. Express* 26 (19) (2018) 24318–24328.
- [3] X. Yin, L. Dong, H. Wu, M. Gao, L. Zhang, X. Zhang, L. Liu, X. Shao, F.K. Tittel, Compact QEPAS humidity sensor in SF<sub>6</sub> buffer gas for high-voltage gas power systems, *Photoacoustics* 25 (2022), 100319.
- [4] Z. Wang, Q. Wang, J.Y.-L. Ching, J.C.-Y. Wu, G. Zhang, W. Ren, A portable low-power QEPAS-based CO<sub>2</sub> isotope sensor using a fiber-coupled interband cascade laser, *Sens. Actuators B: Chem.* 246 (2017) 710–715.
- [5] L. Dong, A.A. Kosterev, D. Thomazy, F.K. Tittel, QEPAS spectrophones: design, optimization, and performance, *Appl. Phys. B* 100 (3) (2010) 627–635.
- [6] Y. Ma, Review of recent advances in QEPAS-based trace gas sensing, *Appl. Sci.* 8 (10) (2018).
- [7] P. Patimisco, A. Sampaolo, L. Dong, F.K. Tittel, V. Spagnolo, Recent advances in quartz enhanced photoacoustic sensing, *Appl. Phys. Rev.* 5 (1) (2018).
- [8] A.A. Kosterev, Y.A. Bakhirkin, R.F. Curl, F.K. Tittel, Quartz-enhanced photoacoustic spectroscopy, *Opt. Lett.* 27 (21) (2002) 1902–1904.
- [9] R. Cui, H. Wu, L. Dong, W. Chen, F.K. Tittel, Multiple-sound-source-excitation quartz-enhanced photoacoustic spectroscopy based on a single-line spot pattern multi-pass cell, *Appl. Phys. Lett.* 118 (16) (2021).
- [10] N. Petra, J. Zweck, A.A. Kosterev, S.E. Minkoff, D. Thomazy, Theoretical analysis of a quartz-enhanced photoacoustic spectroscopy sensor, *Appl. Phys. B* 94 (4) (2009) 673–680.
- [11] Y. Ma, S. Qiao, P. Patimisco, A. Sampaolo, Y. Wang, F.K. Tittel, V. Spagnolo, In-plane quartz-enhanced photoacoustic spectroscopy, *Appl. Phys. Lett.* 116 (6) (2020).
- [12] Z. Li, Z. Wang, Y. Qi, W. Jin, W. Ren, Improved evanescent-wave quartz-enhanced photoacoustic CO sensor using an optical fiber taper, *Sens. Actuators B: Chem.* 248 (2017) 1023–1028.
- [13] Z. Shang, H. Wu, S. Li, G. Wang, A. Sampaolo, P. Patimisco, V. Spagnolo, L. Dong, Ppb-level mid-IR quartz-enhanced photoacoustic sensor for sarin simulant detection using a T-shaped tuning fork, *Sens. Actuators B: Chem.* 390 (2023).
- [14] H. Zheng, H. Lin, L. Dong, Z. Huang, X. Gu, J. Tang, L. Dong, W. Zhu, J. Yu, Z. Chen, Quartz-enhanced photothermal-acoustic spectroscopy for trace gas analysis, *Appl. Sci.* 9 (19) (2019).
- [15] S.D. Russo, A. Zifarelli, P. Patimisco, A. Sampaolo, T. Wei, H. Wu, L. Dong, V. Spagnolo, Light-induced thermo-elastic effect in quartz tuning forks exploited as a photodetector in gas absorption spectroscopy, *Opt. Express* 28 (13) (2020) 19074–19084.
- [16] S. Qiao, Y. He, Y. Ma, Trace gas sensing based on single-quartz-enhanced photoacoustic-photothermal dual spectroscopy, *Opt. Lett.* 46 (10) (2021) 2449–2452.
- [17] Y. Ma, C. Zheng, L. Hu, K. Zheng, F. Song, Y. Zhang, Y. Wang, F.K. Tittel, High-robustness near-infrared methane sensor system using self-correlated heterodyne-based light-induced thermoelastic spectroscopy, *Sens. Actuators B: Chem.* 370 (2022).
- [18] T. Wei, A. Zifarelli, S. Dello Russo, H. Wu, G. Menduni, P. Patimisco, A. Sampaolo, V. Spagnolo, L. Dong, High and flat spectral responsivity of quartz tuning fork used as infrared photodetector in tunable diode laser spectroscopy, *Appl. Phys. Rev.* 8 (4) (2021).
- [19] B. Sun, P. Patimisco, A. Sampaolo, A. Zifarelli, V. Spagnolo, H. Wu, L. Dong, Light-induced thermoelastic sensor for ppb-level H<sub>2</sub>S detection in a SF<sub>6</sub> gas matrices exploiting a mini-multi-pass cell and quartz tuning fork photodetector, *Photoacoustics* 33 (2023).
- [20] Y. Ma, Recent advances in QEPAS and QEPTS based trace gas sensing: a review, *Front. Phys.* 8 (2020).
- [21] Y. Ma, Y. Hu, S. Qiao, Y. He, F.K. Tittel, Trace gas sensing based on multi-quartz-enhanced photothermal spectroscopy, *Photoacoustics* 20 (2020), 100206.
- [22] H. Wu, L. Dong, H. Zheng, Y. Yu, W. Ma, L. Zhang, W. Yin, L. Xiao, S. Jia, F. K. Tittel, Beat frequency quartz-enhanced photoacoustic spectroscopy for fast and calibration-free continuous trace-gas monitoring, *Nat. Commun.* 8 (2017), 15331.
- [23] H. Wu, L. Dong, X. Yin, A. Sampaolo, P. Patimisco, W. Ma, L. Zhang, W. Yin, L. Xiao, V. Spagnolo, S. Jia, Atmospheric CH<sub>4</sub> measurement near a landfill using an ICL-based QEPAS sensor with V-T relaxation self-calibration, *Sens. Actuators B: Chem.* 297 (2019).
- [24] H. Wu, A. Sampaolo, L. Dong, P. Patimisco, X. Liu, H. Zheng, X. Yin, W. Ma, L. Zhang, W. Yin, V. Spagnolo, S. Jia, F.K. Tittel, Quartz enhanced photoacoustic H<sub>2</sub>S gas sensor based on a fiber-amplifier source and a custom tuning fork with large prong spacing, *Appl. Phys. Lett.* 107 (11) (2015).
- [25] Y. Ma, Y. He, Y. Tong, X. Yu, F.K. Tittel, Quartz-tuning-fork enhanced photothermal spectroscopy for ultra-high sensitive trace gas detection, *Opt. Express* 26 (24) (2018) 32103–32110.
- [26] Y. Hu, S. Qiao, Y. He, Z. Lang, Y. Ma, Quartz-enhanced photoacoustic-photothermal spectroscopy for trace gas sensing, *Opt. Express* 29 (4) (2021) 5121–5127.



**Ruyue Cui** received her dual Ph.D. degrees in physics from Shanxi University, China, and Université du Littoral Côte d'Opale, France, in 2023. Currently, she is a lecturer at the Institute of Laser Spectroscopy at Shanxi University. Her research interests encompass optical sensors and laser spectroscopy techniques.



**Hongpeng Wu** received his Ph.D. degree in atomic and molecular physics from Shanxi University, China, in 2017. From 2015–2016, he studied as a joint Ph.D. student in the electrical and computer engineering department and Rice Quantum Institute, Rice University, Houston, USA. Currently he is a professor in the Institute of Laser Spectroscopy of Shanxi University. His research interests include optical sensors and laser spectroscopy techniques.



**Frank K. Tittel** received the B. S., M. S., and Ph. D. degrees in physics from the University of Oxford, Oxford, U.K., in 1955 and 1959, respectively. From 1959–1967, he was a Research Physicist with General Electric (GE) Research and Development Center, Schenectady, NY. At GE, he carried out early pioneering studies of dye lasers and high power solid state lasers. Since 1967, he has been on the faculty of the Department of Electrical and Computer Engineering at Rice University in Houston, TX, where is currently an Endowed Chair Professor. In 1973 and 1981, he was an Alexander von Humboldt Senior Fellow at the Max-Planck Institutes of Biophysical Chemistry, Göttingen, and Quantum Optics, Munich, respectively. He held visiting professor appointments at NASA Goddard Space Flight

Center, University of Aix-Marseille, Keio University (Japan), and Swiss Institute of Technology (ETH-Zurich). Current research interests include various aspects of quantum electronics, in particular laser spectroscopy, nonlinear optics, and laser applications in environmental monitoring, process control, and medicine. He has published more than 300 technical papers and holds seven U.S. patents in these areas.



**Vincenzo Spagnolo** obtained the PhD in physics in 1994 from University of Bari. From 1997–1999, he was researcher of the National Institute of the Physics of Matter. Since 2004, he works at the Technical University of Bari, formerly as assistant and associate professor and, starting from 2018, as full Professor of Physics. Since 2019, he is vice-rector of the Technical University of Bari, deputy to technology transfer. He is the director of the joint-research lab PolySense between Technical University of Bari and THORLABS GmbH, fellow member of SPIE and senior member of OSA. His research interests include optoacoustic gas sensing and spectroscopic techniques for real-time monitoring. His research activity is documented by more than 220 publications and two filed patents. He has given more than 50 invited presentations at international conferences and workshops.

Center, University of Aix-Marseille, Keio University (Japan), and Swiss Institute of Technology (ETH-Zurich). Current research interests include various aspects of quantum electronics, in particular laser spectroscopy, nonlinear optics, and laser applications in environmental monitoring, process control, and medicine. He has published more than 300 technical papers and holds seven U.S. patents in these areas.



**Weidong Chen** obtained his PhD degree from University of Sciences & Technologies of Lille (USTL) in France. He has been on the faculty at University of the Littoral Opal Coast (France) in 1993 as Lecturer and became full Professor of Optics in 2003. He is adjunct faculty of Rice University (USA) and invited professor of Anhui Institute of Optics and Fine Mechanics (Chinese Academy of Sciences, China). His current research interests include: (1) Developments of photonic instrumentation for applied spectroscopy; (2) Optical sensing and metrology of atmospheric species: trace gases (concentration, isotope ratios, vertical concentration profile) and aerosols (optical properties); (3) Optical parametric laser source generation by frequency conversion. He has authored/co-authored more than 160 peer-reviewed articles in scientific journals, conference proceedings and books. He has over 220 conference contributions (including invited conferences oral and poster presentations) and seminars.

Center, University of Aix-Marseille, Keio University (Japan), and Swiss Institute of Technology (ETH-Zurich). Current research interests include various aspects of quantum electronics, in particular laser spectroscopy, nonlinear optics, and laser applications in environmental monitoring, process control, and medicine. He has published more than 300 technical papers and holds seven U.S. patents in these areas.



**Lei Dong** received his Ph.D. degree in optics from Shanxi University, China, in 2007. From June, 2008 to December, 2011, he worked as a post-doctoral fellow in the Electrical and Computer Engineering Department and Rice Quantum Institute, Rice University, Houston, USA. Currently he is a professor in the Institute of Laser Spectroscopy of Shanxi University. His research activities research activities are focused on research and development in laser spectroscopy, in particular photoacoustic spectroscopy applied to sensitive, selective and real-time trace gas detection, and laser applications in environmental monitoring, chemical analysis, industrial process control, and medical diagnostics. He has published more than 100 peer reviewed papers with >2200 positive citations.

Ruyue Cui<sup>1</sup>

*State Key Laboratory of Quantum Optics and Quantum Optics Devices,  
Institute of Laser Spectroscopy, Shanxi University, Taiyuan 030006, China  
Collaborative Innovation Center of Extreme Optics, Shanxi University,  
Taiyuan 030006, China  
Laboratoire de Physicochimie de l'Atmosphère, Université du Littoral Côte  
d'Opale, Dunkerque 59140, France*

Hongpeng Wu<sup>\*2</sup>

*State Key Laboratory of Quantum Optics and Quantum Optics Devices,  
Institute of Laser Spectroscopy, Shanxi University, Taiyuan 030006, China  
Collaborative Innovation Center of Extreme Optics, Shanxi University,  
Taiyuan 030006, China*

Frank K. Tittel

*Department of Electrical and Computer Engineering, Rice University, 6100  
Main Street, Houston, TX 77005, USA*

Vincenzo Spagnolo

*State Key Laboratory of Quantum Optics and Quantum Optics Devices,  
Institute of Laser Spectroscopy, Shanxi University, Taiyuan 030006, China  
PolySense Lab-Dipartimento Interateneo di Fisica, University and Politecnico  
of Bari, Via Amendola 173, Bari, Italy*

Weidong Chen

*Laboratoire de Physicochimie de l'Atmosphère, Université du Littoral Côte  
d'Opale, Dunkerque 59140, France*

Lei Dong<sup>\*</sup>

*State Key Laboratory of Quantum Optics and Quantum Optics Devices,  
Institute of Laser Spectroscopy, Shanxi University, Taiyuan 030006, China  
Collaborative Innovation Center of Extreme Optics, Shanxi University,  
Taiyuan 030006, China*

<sup>\*</sup> Corresponding author.

<sup>\*</sup> Corresponding author.

E-mail address: [wuhp@sxu.edu.cn](mailto:wuhp@sxu.edu.cn) (H. Wu).

E-mail address: [donglei@sxu.edu.cn](mailto:donglei@sxu.edu.cn) (L. Dong).

<sup>1</sup> These authors contributed equally to this work.

<sup>2</sup> These authors contributed equally to this work.